THE JOURNAL OF PHYSICAL CHEMISTRY B

Article

pubs.acs.org/JPCB

Dynamical Stability and Assembly Cooperativity of β-Sheet Amyloid Oligomers − Effect of Polarization

Yang Li,[†] Changge Ji,[†,‡,*] Weixin Xu,[†,‡,*] and John Z.H. Zhang[†,‡,§,*]

[†]State Key Laboratory of Precision Spectroscopy and Department of Physics, Institute of Theoretical and Computational Science, East China Normal University, Shanghai, China

[‡]Institutes for Advanced Interdisciplinary Research, East China Normal University, Shanghai, China

[§]Department of Chemistry, New York University, New York, New York 10003, United States

ABSTRACT: The soluble intermediate oligomers of amyloidogenic proteins are suspected to be more cytotoxic than the mature fibrils in neurodegenerative disorders. Here, the dynamic stability and assembly cooperativity of a model oligomer of human islet amyloid polypeptide (hIAPP) segments were explored by means of all-atom molecular dynamics (MD) simulations under different force fields including AMBER99SB, OPLS, and polarized protein-specific charge (PPC) model. Simulation results show that the dynamic stability of β-sheet oligomers is seriously impacted by electrostatic polarization. Without inclusion of polarization (simulation under standard AMBER and OPLS force field), the β-sheet oligomers are dynamically unstable during MD simulation. For comparison, simulation results under PPC give significantly more stable dynamical structures of the oligomers. Furthermore, calculation of electrostatic interaction energy between the neighboring β strands with an approximate polarizable method produces energetic evidence for cooperative assembly of β-strand oligomers. This result supports a picture of downhill-like cooperative assembly of β strands during fibrillation process. The present study demonstrates the critical role of polarization in dynamic stability and assembly cooperativity of β-sheet-rich amyloid oligomers.

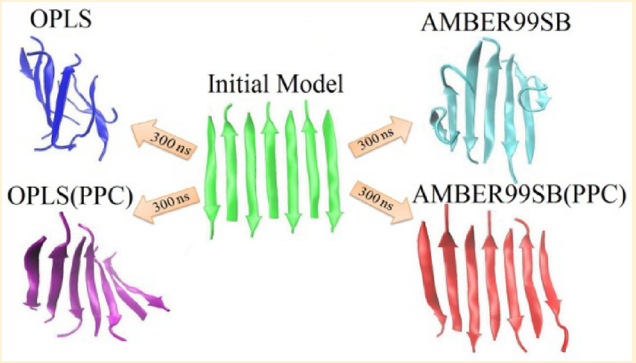

1. INTRODUCTION

Amyloidal fibrils formed by amyloidogenic proteins, such as hIAPP, amyloid-β peptide, α-synuclein,[1] are linked to several neurodegenerative diseases including type 2 diabetes mellitus, Alzheimer's, and prion diseases. Recently, more and more experimental evidence suggested that the soluble intermediate oligomers are the most cytotoxic forms of amyloidogenic proteins, and the interactions of these soluble oligomers with lipid membranes may play an important role in the pathogenesis of amyloid disease.[2−7] Thus, investigation of the structural features and interaction dynamics of the toxic oligomers of amyloidogenic proteins or peptides should help understand the potential assembly mechanisms and provide insights for designing new strategy to prevent the formation and accumulation of these amyloid soluble oligomers.

Besides experimental measurements, molecular dynamics simulations have played indispensable roles in studying the structural dynamics of single proteins[8−11] and exploring the assembly dynamics of amyloidogenic proteins or peptides,[12−19] which are not always easily accessible by experiments. Nevertheless, the success of mechanism prediction by MD simulations is somewhat hindered by the inaccuracy of the existing force fields, especially when dealing with structures owning an abundant hydrogen bond network that plays an essential role in secondary structures of proteins. Our recent work has demonstrated that electrostatic polarization stabilizes intraprotein hydrogen bonds and proteins' local structures near the native state of proteins.[20,21] It is noted that the framework of hIAPP amyloid aggregates is mainly stabilized by the rich backbone hydrogen bonding network. It is therefore conjectured that electrostatic polarization, particularly in hydrogen bonding, may help characterize the conformation dynamics and assembly mechanism of hIAPP aggregates.

In this study, we investigate the effect of electrostatic polarization on structural stability, conformation dynamics, and assembly cooperativity of the model antiparallel β-sheets of hIAPP segments[22] in an aqueous environment. We carried out a series of all-atom MD simulations at room temperature using respectively the standard AMBER99SB force field,[23] the all-atom OPLS force field,[24] and the polarized protein-specific charge (PPC) model.[25] The PPC was derived from quantum mechanical calculation for protein using a fragment approach (MFCC-PB).[26−30] Thus, PPC is protein specific, which sets it apart from amino acid-specific charges used in the standard force fields. The purpose of our study is 2-fold. (1) What is the effect of polarization on dynamical stability of amyloidogenic

Received: August 31, 2012
Revised: October 19, 2012
Published: October 25, 2012

   dx.doi.org/10.1021/jp3086599 | J. Phys. Chem. B 2012, 116, 13368−13373

oligomers composed of different number of β strands? (2) Is there any cooperative effect in assembly dynamics or aggregation of these oligomers due to polarization? To address these questions, MD simulations will be carried out under several force fields, both nonpolarizable and polarized ones.

2. METHODS

Initial Structures. Our theoretical study was initiated from a model antiparallel β-sheet based on experimental observation. This system is comprised of seven identical strands (Figure 1)

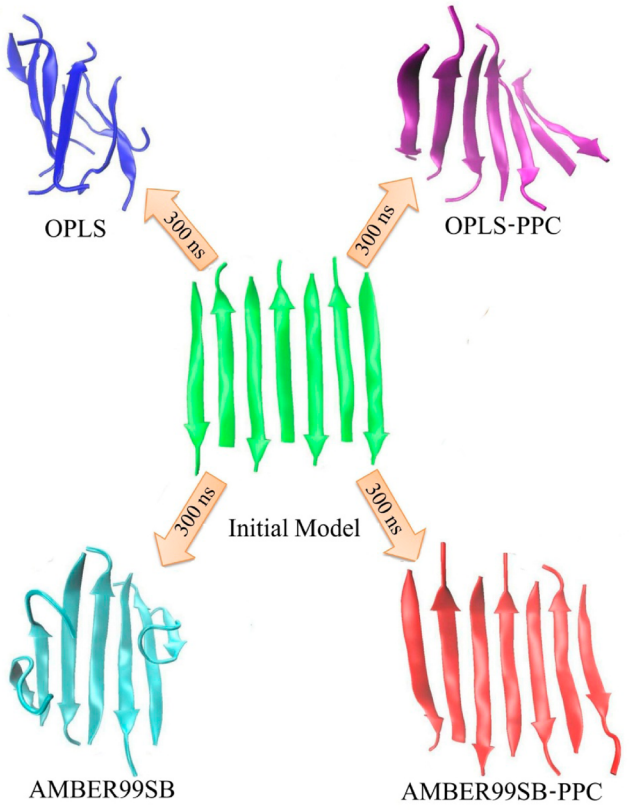

Figure 1. Initial structure of the 7-strand β-sheet with seven identical strands spaced ~4.7 Å apart in an antiparallel organization. Each strand consists of a hIAPP20−29 segment (ACE-SNNFGAILSS-NME). The final structure from MD simulation (300 ns) under respectively the OPLS (blue), OPLS-PPC (purple), AMBER99SB (cyan), and AMBER99SB-PPC (red) force fields.

and each strand consists of a hIAPP20−29 segment (ACE-SNNFGAILSS-NME). The properties of this segment are similar to those of a full-length hIAPP, and membrane fragmentation induced by the aggregation of this short peptide segment has been observed.[31,32] The orientation of the interstrands was organized in an antiparallel manner based on experimental observations.[33,34] In addition, we extracted the first two, three, four, and five strands from the system to study their dynamic stabilities (details for simulation setup are shown in Table 1).

Generation of PPC. To study the effect of polarization on dynamical stability and assembly cooperativity, it is necessary to employ a polarized or polarizable force field. In the current study, we employed a polarized protein-specific force field (PPC) in MD simulations. Because the procedure to compute PPC for a given protein structure is already reported

Table 1. Details of All Simulations[a]

runs	system	method (force field)	time (ns)	water
run1	7 strands	OPLS	300	30 303
run2	7 strands	OPLS(PPC)	300	30 303
rnu3	7 strands	AMBER99SB	300	30 303
run4	7 strands	AMBER99SB-PPC	300	30 303
run5	2 strands	AMBER99SB	300	22 593
run6	2 strands	AMBER99SB-PPC	300	22 593
run7	3 strands	AMBER99SB	300	22 464
run8	3 strands	AMBER99SB-PPC	300	22 464
run9	4 strands	AMBER99SB	300	25 146
run10	4 strands	AMBER99SB-PPC	300	25 146
run11	5 strands	AMBER99SB	300	25 026
run12	5 strands	AMBER99SB-PPC	300	25 026

[a]We carried out twelve MD simulations in total, using five systems including the whole seven strands, the first two, three, four, and five strands. The system of seven strands separately uses OPLS force field, AMBER99SB force field, and then both of them are replaced by PPC. The other systems just use the AMBER99SB force field and PPC. The numbers of water are listed in the table.

elsewhere,[25,35] only a brief outline is given here. The basic procedure is as follows: First, gas phase quantum chemistry calculation of protein is performed with a fragment quantum mechanical approach to obtain initial electron density of the protein for a given protein structure.[26,36] The calculated electron density is used to fit atomic charges using the RESP.[37] Solution of the Poison-Boltzmann (PB) equation is then carried out to obtain the reaction field due to the presence of solvent and the discrete surface charges on the cavity surface are generated. Then new quantum mechanical calculation of the protein is performed again in the external field of the induced surface charges. The procedure is repeated until convergence is reached.

MD Protocol. All MD simulations were performed using the *GROMACS* software package[38] at T = 300 K. Each system was solvated with explicit SPC water molecules in cubic boxes of various sizes ranging from 61 to 69 Å. Following energy minimization using the steepest descent, two 100 ps equilibration runs were conducted under NVT and NPT ensembles, separately, to obtain the correct temperature and proper density. The protein and water molecules were separately coupled to an external heat bath with a relaxation time of 0.1 ps. All bonds involving hydrogen atoms were constrained in length according to LINCS protocol.[39] A time step of 2 fs was used and the trajectories were saved every 2 ps for analysis. The particle mesh Ewald method[40] with a 10 Å cutoff was used for electrostatic interaction, and, for van der Waals interactions, a cutoff of 12 Å was used. In our current study, two types of MD simulations were carried out: simulations using the standard OPLS or AMBER99SB force field and the corresponding simulations using the PPC (details in Table 1). In simulations using PPC, the charges in OPLS or AMBER99SB were simply replaced with the PPC, whereas the other parameters of the force fields were retained.

3. RESULT AND DISCUSSION

3.1. Seven-Strand β-Sheet Oligomer. *Conformational Distortion.* The conformation dynamics of a seven-strand β-sheet was studied first by MD simulation, in which four separate runs were carried out using respectively the OPLS, OPLS-PPC, AMBER99SB and AMBER99SB-PPC force fields.

dx.doi.org/10.1021/jp3086599 | J. Phys. Chem. B 2012, 116, 13368−13373

Figure 1 displays the final structures of the β-sheet at 300 ns under different force fields. The final structures under standard OPLS and AMBER99SB force fields are both bended and distorted, whereas the others using OPLS-PPC and AMBER99SB-PPC are more stable and ordered, especially the one using AMBER99SB-PPC. In this sense, the AMBER force field seems more suitable for MD simulation than the OPLS force field for the seven-strand β-sheet system.

The overall extent of conformational distortion with respect to the initial conformation can be measured by root-mean-square deviation (RMSD) of backbone atoms. The comparison among simulated structures in Figure 1 and RMSDs in Figure 2

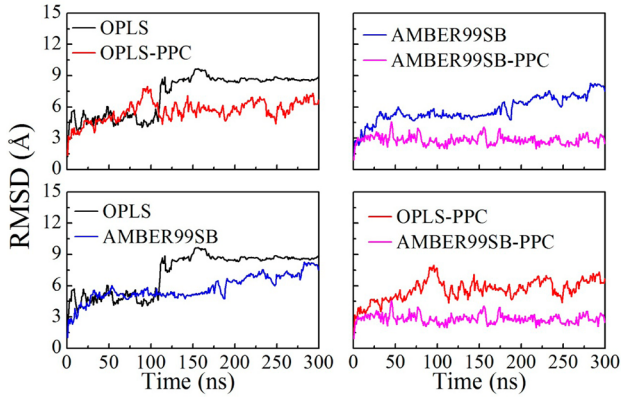

Figure 2. Backbone RMSD values of the seven-strand β-sheet as a function of time for MD simulations using, respectively, OPLS (black), AMBER99SB (blue), OPLS-PPC (red), and AMBER99SB-PPC (purple) force fields at 300K.

indicates clearly that the AMBER99SB force field preserves the structural integrity of the β-sheet better and is therefore more suitable for simulation study of β-sheet amyloid system than the OPLS force field. Further comparison of the results between nonpolarizable force fields and PPC in Figure 1 and Figure 2 shows that polarization plays a significant role in preserving the stable structure of the β-sheet system in MD simulation. In particular, we noticed that RMSD of the system under AMBER99SB-PPC remains under 3 Å throughout the simulation time of 300 ns.

Effect of Polarization on Hydrogen-Bonding Strength. The hydrogen bond (H-bond) network, which is dominated by electrostatic interactions, plays an essential role in maintaining secondary structures of proteins. PPC was shown to correctly describe the polarized electrostatic state of proteins at given structures.[20] So we expect that electrostatic polarization effect would also play a role in the H-bond network of the hIAPP oligomer. To quantitatively verify it, we analyzed the time evolution of H-bond number and length during simulations. As shown in part A of Figure 3, the number of H-bonds under the AMBER99SB force field gradually decreases from an initial value of 53 to 39, whereas the number remains quite steady at around 50 under AMBER99SB-PPC. This indicates that some H-bonds are broken under the AMBER99SB force field without considering the polarization effect. For example, the H-bond length between ASN3 and LEU21, plotted as a function of simulation time in part B of Figure 3, shows that the H-bond breaks after about 140 ns under the AMBER99SB force field. In contrast, the same H-bond is still very stable under PPC. Thus, PPC stabilizes the β-sheet by forming a more steadier hydrogen

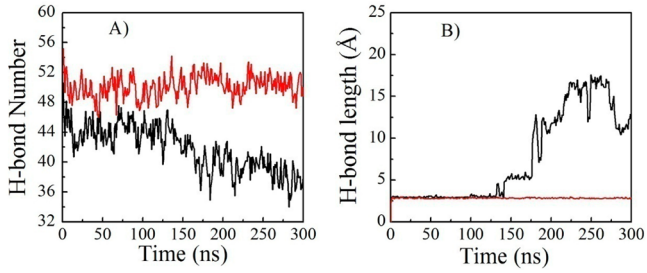

Figure 3. (A) Number of hydrogen bond as a function of simulation time. (B) Time evolution of the hydrogen bond length between ASN3 and LEU21 during MD simulation. The black line is under AMBER99SB force field and the red line is under AMBER99SB-PPC.

bond network through the effect of polarization that strengthens the hydrogen bonds in β-sheet structures.

3.2. Other β-sheet Oligomers. Amyloid fibril grows by adding free monomers onto existing amyloid nucleus of small oligomers.[41−44] In the above, we have discussed the structural stability of a single β-sheet composed of seven monomers under different force fields. In the following, we explore the role of electrostatic polarization by modeling smaller oligomers of β-sheets including two, three, four, and five strands. For this purpose, we carried out a series of 300 ns simulations under, separately, the AMBER99SB and AMBER99SB-PPC force fields employing the same MD protocol as above. The details of these MD runs are listed in Table 1. Again we extracted the final equilibrated structures (Figure 4), and calculated the RMSD with respect to the initial structures from the MD trajectories (Figure 5). By visually comparing the equilibrated structures with initial structures, we can see that the structures using PPC are significantly more stable than those under the

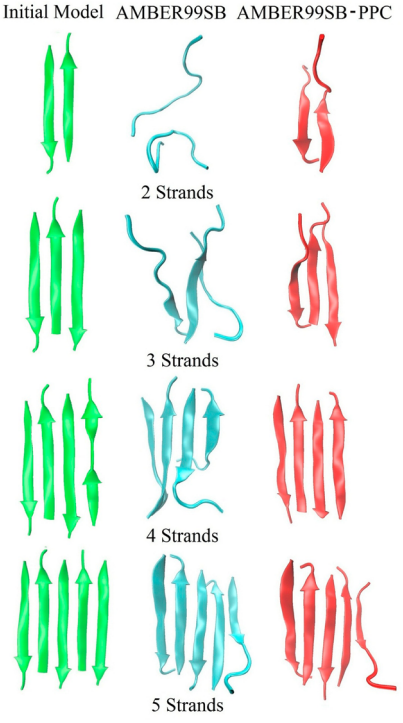

Figure 4. Initial structure (green) and the final structure from MD simulation (300 ns) under respectively AMBER99SB (cyan) and AMBER99SB-PPC (red) force field.

dx.doi.org/10.1021/jp3086599 | J. Phys. Chem. B 2012, 116, 13368−13373

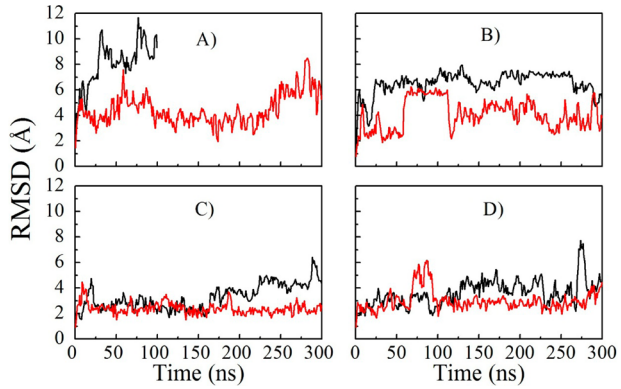

Figure 5. Backbone RMSD of various β-sheet oligomers as a function of time for MD simulations under AMBER99SB (black) and AMBER99SB-PPC (red) at 300K. (A), (B), (C), (D) are respectively for 2 strands, 3 strands, 4 strands, 5 strands.

pure AMBER99SB force field. And it is noticed that the RMSD under pure AMBER99SB force field is obviously larger than that under PPC. Therefore, we further demonstrated that the polarization effect is important in stabilizing the β-sheet with different strands.

3.3. Assembly Cooperativity of the β Strands. We further investigate the polarization effect on the assembly cooperativity of the β strands. By assembly cooperativity, we mean that interstand binding interaction is enhanced with the growth of system by adding more β strands to the system. This is done by adding more β strands to the system while keeping the original β sheet rigid. This is carried out using two approaches. In the first approach, the initial system consists of just two β strands (strand 1 and 2) and their interstrand electrostatic interaction energy is calculated. The calculation of this interaction energy is repeated again whenever an additional β strand is added toward its right side up to a total of 7 β strands. In the second approach, the initial system also consists of just two β strands (strand 3 and 4) and their interstrand electrostatic interaction energy is again calculated similarly. But the additional β strands were added to the system from both sides simultaneously to grow the system, for example, the system grows from consisting of just 3−4 strands to 2−3−4−5 and 1−2−3−4−5−6 strands.

We should note here that because the relative geometry of the first two strands in both approaches (1 and 2 in the first approach and 3 and 4 in the second approach) are fixed, the calculated interstrand electrostatic interaction energy would be independent of the addition of β strands to the sides in the standard nonpolarizable force field such as AMBER99SB. Correct calculation of this energy change requires the use of a reasonably reliable polarizable force field and a proper formula for the corresponding electrostatic interaction (EI) energy calculation. In the following, we describe a simple approach to obtain a reasonable estimate of the EI. Our focus is on the estimate of relative EI when additional strands are added to the original 2-strand system.

For each pair of interstrand atoms, we assume that their initial atomic charges are q_{10} and q_{20} in the unassociated state (two strands are infinitely separated), and their final charges are q_1 and q_2 in the associated state (two strands in the initial separation). Here, the q_{10} and q_{20} are calculated using the method described in the method section. Because of polarization, the q_1 and q_2 are recalculated when the environment is changed, e.g., when an additional β strand is present next to it. The EI between each atom pair is calculated by the following method:

$$\begin{aligned} \mathrm{EI} &= -\int_{\infty}^{r} \frac{(q_1 q_2)}{r^2}\mathrm{d}r \\ &= -\int_{\infty}^{r} \frac{(q_{10}+\Delta q_1)(q_{20}+\Delta q_2)}{r^2}\mathrm{d}r \end{aligned} \quad (1)$$

Where

$$q_1 = q_{10} + \Delta q_1,\ q_2 = q_{20} + \Delta q_2$$

$$\Delta q_1 = \frac{\alpha}{r},\ \Delta q_2 = \frac{\beta}{\gamma}$$

Then, EI (1) can be integrated to give:

$$\begin{aligned} \mathrm{EI} &= \frac{q_{10}q_{20}}{r} + \frac{q_{10}\Delta q_2}{2r} + \frac{q_{20}\Delta q_1}{2r} + \frac{\Delta q_1 \Delta q_2}{3r} \\ &= \frac{q_{10}q_{20}}{r} + \frac{q_1\Delta q_2}{2r} + \frac{q_2\Delta q_1}{2r} - \frac{2\Delta q_1\Delta q_2}{3r} \\ &\approx \frac{q_{10}q_{20}}{r} + \frac{1}{2}\left(\frac{q_1 q_2}{r} - \frac{q_{10}q_{20}}{r}\right) \\ &= \frac{1}{2}\left(\frac{q_1 q_2}{r} + \frac{q_{10}q_{20}}{r}\right) \end{aligned} \quad (2)$$

Growth of β Strand from One Side. We calculated the EI energy between the first and second strands for the two (1−2), three (1−2−3), four (1−2−3−4), five (1−2−3−4−5), six (1−2−3−4−5−6), and seven-strand (1−2−3−4−5−6−7) systems using PPC. The experimental crystal structure of the seven-strand system is used as the initial structure and is optimized with AMBER force field. The other structures are obtained by simply taking away other strands to obtain the proper number of strands (2 to 7). Because the relative structure of the two-strand system (1 and 2) is fixed in various oligomers, the change of EI between the first and second strand solely reflects the effect of polarization. It is important to note in Table 2 that the EI energy (attractive interaction) between the first and the second strand is increased by an appreciable amount (~0.3 kcal/mol) with the addition of the third strand to its side. Adding additional strand to the same side gives only a tiny increase of EI (~0.04 kcal/mol), simply because it is further away from the first two strands. Part A of Figure 6 shows the profile of EI between the first two strands as additional strands is added toward the same side. As is seen from part A of Figure

Table 2. Electrostatic Interaction (EI) Energy (kcal/mol) between the First and Second β-Strand in Systems Ranging from 2 to 7 Strands

no. of β-strand	[1−2]	[1−2]-3	[1−2]-3−4	[1−2]-3−4−5	[1−2]-3−4−5−6	[1−2]-3−4−5−6−7
EI Energy	−80.645	−80.964	−80.999	−81.019	−80.973	−81.047
ΔEI Energy	0	−0.319	−0.354	−0.374	−0.328	−0.402

dx.doi.org/10.1021/jp3086599 | J. Phys. Chem. B 2012, 116, 13368−13373

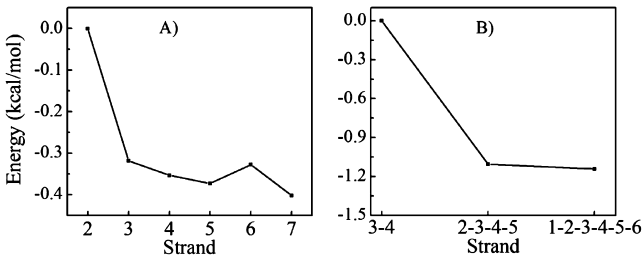

Figure 6. (A) Difference in electrostatic interaction energy between the two neighboring β strands (1 and 2) as more strands are added to the same side (up to a total of 7 strands). (B) Difference in electrostatic interaction energy between the two neighboring β strands (3 and 4) as more strands are added to both sides (up to a total of 6 strands).

6, the major effect of polarization is due to the presence of the nearest neighbor strand.

Growth of β Strand from Both Sides. We similarly calculated the EI energy between the third and fourth strands for oligomers with 3−4, 2−3−4−5, and 1−2−3−4−5−6 strands, that is, with the additional strands growing from both sides. As in the way above, the relative structure of the two-strand system (3 and 4) is fixed in various oligomers, the change of EI between the third and forth strand solely reflects the effect of polarization. Table 3 lists the EI energies, which

Table 3. Electrostatic Interaction Energy (kcal/mol) between the Two Middle (3 and 4) β-Strand in Systems Consisting of 3-4, 2-3-4-5, and 1-2-3-4-5-6 Strands

no. of β-strands	[3−4]	2-[3−4]-5	1−2-[3−4]-5−6
EI Energy	−65.521	−66.626	−66.662
ΔEI Energy	0	−1.105	−1.141

clearly shows that the EI energy is obviously increased with the growth of β strands from both sides. Here, it is interesting to note that when adding the second and fifth strands to the two-strand system (3−4), the EI energy (attractive interaction) between the third and fourth strands is increased by an appreciable amount (∼1.1 kcal/mol), which is about three times of the value that adding strands only from one side (as shown in the above section). This reflects a stronger polarization effect from two nearest neighboring strands. As continuing to add strands from both sides, it gives only a tiny increase of EI (∼0.04 kcal/mol), which is nearly the same as just adding strands from one side, simply because it is further away from the first two strands. It again indicates that the short-range polarization plays a key role in the growth of β strands. In all, the variation of EI energy for different systems is indeed cooperative during the assembly of the hIAPP amyloid oligomer.

4. CONCLUSIONS

In this article, the dynamical stability and assembly cooperativity of a model oligomer of human islet amyloid polypeptide (hIAPP) segments were studied by all-atom molecular dynamics (MD) simulations under both standard nonpolarizable force fields and polarized protein-specific charge (PPC) model. Simulation results show that dynamical stability of β-sheet oligomers is seriously impacted by electrostatic polarization. Without inclusion of polarization in the force field, the β-sheet oligomers are dynamically unstable during MD simulation. For comparison, simulation under PPC gives significantly more stable dynamical structures of the oligomers. Furthermore, calculation of electrostatic interaction energy between the neighboring β strands with an approximate polarizable method produces energetic evidence for cooperative assembly of β-strand oligomers. The result thus supports a picture of downhill-like cooperative assembly of β strands during fibrillation process. The present study demonstrates the critical role of polarization in dynamic stability and assembly cooperativity of β-sheet-rich amyloid oligomers.

AUTHOR INFORMATION

Corresponding Author

*E-mail: chicago.ji@gmail.com (C.J.), wxxu@sat.ecnu.edu.cn (W.X.), zhzhang@phy.ecnu.edu.cn (J.Z.H.Z.).

Notes

The authors declare no competing financial interest.

ACKNOWLEDGMENTS

We thank the National Natural Science Foundation of China (Grants No. 21003048, 10974054, 20933002, and 11204083). W.X.X. is grateful to Shanghai Pu Jiang program (12PJ1403000) for financial support. We also thank the Supercomputer Center of ECNU for providing us computational time.

REFERENCES

(1) Sunde, M.; Blake, C. C. F. *Q. Rev. Biophys.* **1998**, *31*, 1−39.
(2) Lambert, M. P.; Barlow, A. K.; Chromy, B. A.; Edwards, C.; Freed, R.; Liosatos, M.; Morgan, T. E.; Rozovsky, I.; Trommer, B.; Viola, K. L.; Wals, P.; Zhang, C.; Finch, C. E.; Krafft, G. A.; Klein, W. L. *Proc. Natl. Acad. Sci. U. S. A.* **1998**, *95*, 6448−6453.
(3) Janson, J.; Ashley, R. H.; Harrison, D.; McIntyre, S.; Butler, P. C. *Diabetes* **1999**, *48*, 491−498.
(4) Hardy, J.; Selkoe, D. J. *Science* **2002**, *297*, 353−356.
(5) Kayed, R.; Head, E.; Thompson, J. L.; McIntire, T. M.; Milton, S. C.; Cotman, C. W.; Glabe, C. G. *Science* **2003**, *300*, 486−489.
(6) Klyubin, I.; Walsh, D. M.; Lemere, C. A.; Cullen, W. K.; Shankar, G. M.; Betts, V.; Spooner, E. T.; Jiang, L. Y.; Anwyl, R.; Selkoe, D. J.; Rowan, M. J. *Nat. Med.* **2005**, *11*, 556−561.
(7) Meier, J. J.; Kayed, R.; Lin, C.-Y.; Gurlo, T.; Haataja, L.; Jayasinghe, S.; Langen, R.; Glabe, C. G.; Butler, P. C. *Am. J. Physiol-Endoc. M.* **2006**, *291*, E1317−E1324.
(8) Xu, W. X.; Lai, T.; Yang, Y.; Mu, Y. *J. Chem. Phys.* **2008**, *128*, 175105.
(9) Mu, Y. G.; Nordenskiold, L.; Tam, J. P. *Biophys. J.* **2006**, *90*, 3983−3992.
(10) Xu, W. X.; Mu, Y. *Biophys. Chem.* **2008**, *137*, 116−125.
(11) Sgourakis, N. G.; Yan, Y. L.; McCallum, S. A.; Wang, C. Y.; Garcia, A. E. *J. Mol. Biol.* **2007**, *368*, 1448−1457.
(12) Jiang, P.; Xu, W. X.; Mu, Y. G. *PLoS Comput. Biol.* **2009**, *5*, e1000357.
(13) Xu, W. X.; Jiang, P.; Mu, Y. *J. Phys. Chem. B* **2009**, *113*, 7308−7314.
(14) Negureanu, L.; Baumketner, A. *J. Mol. Biol.* **2009**, *389*, 921−937.
(15) Nguyen, P. H.; Li, M. S.; Derreumaux, P. *Phys. Chem. Chem. Phys.* **2011**, *13*, 9778−9788.
(16) Gnanakaran, S.; Nussinov, R.; Garcia, A. E. *J. Am. Chem. Soc.* **2006**, *128*, 2158−2159.
(17) Ma, B. Y.; Nussinov, R. *Curr. Opin. Chem. Biol.* **2006**, *10*, 445−452.
(18) Ma, B. Y.; Nussinov, R. *Biophys. J.* **2006**, *90*, 3365−3374.
(19) Li, H. Y.; Luo, Y.; Derreumaux, P.; Wei, G. H. *Biophys. J.* **2011**, *101*, 2267−2276.
(20) Duan, L. L.; Mei, Y.; Zhang, Q. G.; Zhang, J. Z. H. *J. Chem. Phys.* **2009**, *130*, 115102.

(21) Gao, Y.; Lu, X. L.; Duan, L. L.; Zhang, J. Z. H.; Mei, Y. *J. Phys. Chem. B* **2012**, *116*, 549−554.
(22) Xu, W.; Ping, J.; Li, W.; Mu, Y. *J. Chem. Phys.* **2009**, *130*, 164709.
(23) Duan, Y.; Wu, C.; Chowdhury, S.; Lee, M. C.; Xiong, G. M.; Zhang, W.; Yang, R.; Cieplak, P.; Luo, R.; Lee, T.; Caldwell, J.; Wang, J. M.; Kollman, P. *J. Comput. Chem.* **2003**, *24*, 1999−2012.
(24) Jorgensen, W. L. M., D. S.; Tirado-Rives, J. *J. Phys. Chem.* **1996**, *118*, 11225−11236.
(25) Ji, C. G.; Mei, Y.; Zhang, J. Z. H. *Biophys. J.* **2008**, *95*, 1080−1088.
(26) Zhang, D. W.; Zhang, J. Z. H. *J. Chem. Phys.* **2003**, *119*, 3599−3605.
(27) He, X.; Mei, Y.; Xiang, Y.; Zhang, D. W.; Zhang, J. Z. H. *Proteins: Struct. Funct. Bioinform.* **2005**, *61*, 423−432.
(28) Mei, Y.; He, X.; Xiang, Y.; Zhang, D. W.; Zhang, J. Z. H. *Proteins: Struct. Funct. Bioinform.* **2005**, *59*, 489−495.
(29) Barry Honig, K. S.; An Suei, Yang *J. Phys. Chem.* **1993**, *97*, 1101−1109.
(30) Tannor, D. J.; Marten, B.; Murphy, R.; Freisner, R. A.; Sitkoff, D.; Nicholls, A.; Ringnalda, M.; Goddardi, W. A. I.; Honig, B. *J. Am. Chem. Soc.* **1994**, *116*, 11875−11882.
(31) Westermark, P.; Engstrom, U.; Johnson, K. H.; Westermark, G. T.; Betsholtz, C. *Proc. Natl. Acad. Sci. U. S. A.* **1990**, *87*, 5036−40.
(32) Brender, J. R.; Duerr, U. H. N.; Heyl, D.; Budarapu, M. B.; Ramamoorthy, A. *Bba-biomembranes* **2007**, *1768*, 2026−2029.
(33) Ashburn, T. T.; Auger, M.; Lansbury, P. T., Jr. *J. Am. Chem. Soc.* **1992**, *114* (2), 790−791.
(34) Griffiths, J. M.; Ashburn, T. T.; Auger, M.; Costa, P. R.; Griffin, R. G.; Lansbury, P. T., Jr. *J. Am. Chem. Soc.* **1995**, *117* (12), 3539−3546.
(35) Ji, C. G.; Zhang, J. Z. H. *J. Am. Chem. Soc.* **2008**, *130*, 17129−17133.
(36) Ye, M.; Changge, J.; Zhang, J. Z. H. *J. Chem. Phys.* **2006**, *125*, 094906.
(37) Bayly, C. I.; Cieplak, P.; Cornell, W. D.; Kollman, P. A. *J. Phys. Chem.* **1993**, *97*, 10269−10280.
(38) Berendsen, H. J. C.; van der Spoel, D.; van Drunen, R. *Comput. Phys. Commun.* **1995**, *91*, 43−56.
(39) Hess, B.; Bekker, H.; Berendsen, H. J. C.; Fraaije, J. *J. Comput. Chem.* **1997**, *18*, 1463−1472.
(40) Darden, T.; York, D.; Pedersen, L. *J. Chem. Phys.* **1993**, *98*, 10089−92.
(41) Ma, B. Y.; Nussinov, R. *Protein Sci.* **2002**, *11*, 2335−2350.
(42) Fay, N.; Inoue, Y. J.; Bousset, L.; Taguchi, H.; Melki, R. *J. Biol. Chem.* **2003**, *278*, 30199−30205.
(43) Wu, C.; Lei, H. X.; Duan, Y. *Biophys. J.* **2004**, *87*, 3000−3009.
(44) Nguyen, P. H.; Li, M. S.; Stock, G.; Straub, J. E.; Thirumalai, D. *Proc. Natl. Acad. Sci. U. S. A.* **2007**, *104*, 111−116.